Available online at www.sciencedirect.com
SCIENCE DIRECT®
International Journal of Heat and Fluid Flow 24 (2003) 726–735
International Journal of HEAT AND FLUID FLOW
www.elsevier.com/locate/ijhff

Unsteady mixed convection in a horizontal channel with rectangular blocks periodically distributed on its lower wall

M. Najam [a], A. Amahmid [b,*], M. Hasnaoui [b], M. El Alami [a]

[a] Groupe Energétique, Département de Physique, Faculté des Sciences Aïn Chock, Université Hassan II, Casablanca, Morocco
[b] Laboratoire de Mécanique des Fluides et Energétique, Département de Physique, Facultédes Sciences Semlalia, Université Cadi Ayyad, Marrakech, Morocco

Received 15 June 2002; accepted 2 April 2003

Abstract

We present a numerical study of laminar unsteady mixed convection in a two dimensional horizontal channel containing heating blocks periodically mounted on its lower wall while its upper wall is maintained cold at a constant temperature. The flow is assumed to be fully developed and periodic conditions are used in the longitudinal direction of the channel. The parameters governing the problem are the Reynolds number ($0.1 \leqslant Re \leqslant 200$), the Rayleigh number ($10^4 \leqslant Ra \leqslant 10^6$) and the relative height of the blocks ($0.25 \leqslant B = h'/H' \leqslant 0.5$). The effect of the forced flow on the natural convection cells is studied for different values of the governing parameters. The conditions corresponding to the displacement of these cells and the unsteadiness of the flow are determined. The fully developed forced flow is found to reduce considerably the heat transfer through the cold surface of the channel at relatively large *Re*.

Keywords: Unsteady mixed convection; Heat transfer; Horizontal channel; Heated blocks; Periodic conditions; Numerical method

1. Introduction

Mixed convection induced in a channel containing heating elements on one of its walls or on both walls is important from both theoretical and practical points of view. In fact, this configuration can be encountered in various engineering applications, such as in cooling of electronic components and compact heat exchangers. The literature review shows that most of the studies related to the cooling of electronic components are concerned with forced convection. Nevertheless, mixed convection phenomena have received increasing attention due to the important role they may play at low and moderate Reynolds numbers which are appropriate for the cooling of systems with relatively weak power dissipation. Kennedy and Zebib (1983) presented numerical results on laminar mixed convection in a horizontal channel with a heat source placed on the lower or the upper wall. It is found that the last situation will realize temperatures almost twice those obtained when the heat source is located on the lower wall. The mixed convection flow and heat transfer between inclined parallel plates with localized heat sources dissipating a uniform heat flux over their length have been studied numerically by Tomimura and Fujii (1987). The effect of mixed convection, plate inclination and length-to-height ratio were correlated in order to predict the maximum temperature of each heat source. Yücel et al. (1993) studied mixed convection heat transfer in an inclined channel with isothermal discrete heating elements on one side. They found that the heat transfer can be considerably affected by the imposed flow, inclination angle and strength of the natural convection. The mixed convection in a horizontal channel heated periodically from below was considered by Hasnaoui et al. (1991). They reported that for a fixed size of the heated element and a given Rayleigh number, a complicated solution structure can be observed upon increasing the Reynolds number. There is, particularly, a critical value of this parameter above which the natural convection rolls are carried downstream with a time dependent velocity, the flow becoming periodic in time. Kim et al. (1992) studied numerically mixed convection around three obstacles in

* Corresponding author. Fax: 212-44-43-74-10.
E-mail address: amahmid@ucam.ac.ma (A. Amahmid).

0142-727X/$ - see front matter © 2003 Published by Elsevier Inc.
doi:10.1016/S0142-727X(03)00063-8

Nomenclature

A	dimensionless geometric parameter, L'/H'
B	dimensionless geometric parameter, h'/H'
C	dimensionless geometric parameter, d'/H'
g	acceleration due to gravity
h'	height of the blocks
H'	height of channel
d'	spacing between two neighboring blocks
L'	horizontal length of calculation domain
Pe	Peclet number, $RePr$
Pr	Prandtl number, ν/α
Q	average heat quantity, Eq. (5)
Q_m	averaged value of Q over a flow cycle
Ra	Rayleigh number, $g\beta\Delta T'H'^3/(\alpha\nu)$
Re	Reynolds number, $H'u'_0/\nu$
t'	time
T	dimensionless time, $t'/(T'/u'_0)$
T'	temperature of fluid
T	dimensionless temperature, $(T'-T'_C)/(T'_H-T'_C)$
$\Delta T'$	temperature difference, $T'_H-T'_C$
u', v'	velocities in x' and y' directions
u, v	dimensionless velocity in x' and y' directions, $(x', y')/u'_0$
u'_0	characteristic velocity of the forced flow
x', y'	Cartesian coordinates
x, y	dimensionless Cartesian coordinates, $(x', y')/H'$

Greeks

α	thermal diffusivity
β	volumetric coefficient of thermal expansion
ν	kinematic viscosity
Ψ'	stream function
Ψ	dimensionless stream function, $\Psi'/(H'u'_0)$
Ω'	vorticity
Ω	dimensionless vorticity, $\Omega'/(u'_0/H')$

Subscripts

cr	critical
C	cold wall
H	hot wall
max	maximum value
min	minimum value

Superscript

$'$	dimensional variables

horizontal and vertical channels. The local Nusselt number distributions presented for various Gr/Re^2 showed that the heat transfer is higher at the level of the first obstacle. The effect of buoyancy forces on the fluid flow and heat transfer in a horizontal channel containing blocks on its lower or upper wall was studied by Braaten and Patankar (1985). Their analysis was carried out in the case of a laminar flow assuming hydrodynamically and thermally fully-developed conditions in the axial direction of the channel. They concluded that the secondary flow induced by buoyancy leads to a significant enhancement in heat transfer over the forced convection results. Some heat transfer augmentation techniques have also been published in the case of mixed convection flows. For example, Fusegi (1996) studied mixed convection in the case of fully developed flows of air inside a channel subjected to oscillatory pressure gradient. He found that the modifications imposed by mixed convection on the flow structure result in an improvement of the heat transfer compared to that obtained in pure forced convection regime. Wu and Perng (1998) analyzed unsteady mixed convection flow and heat transfer characteristics in a vertical block-heated channel when vortex shedding is produced following the use of an inclined plate above an upstream block. They concluded that this technique leads effectively to the improvement of the heat transfer in the channel by modifying the flow structure.

In the present paper, a numerical study of mixed convection in a two dimensional horizontal channel with isothermal heating blocks periodically mounted on its lower wall is carried out. The forced flow is assumed to be fully developed in the longitudinal direction to apply the periodic conditions. The main objective of this study is to analyze the effect of the forced flow on the natural convection cells and also on the steady and unsteady nature of the flow for various blocks heights. It is demonstrated that the natural convection cells are moving downstream with periodic velocities above critical Reynolds numbers which will be presented as functions of Ra.

2. Mathematical model

The system under consideration is a two dimensional horizontal channel containing heating blocks regularly distributed on its lower adiabatic wall and maintained at a constant temperature T'_H (Fig. 1). The upper wall of the channel is maintained at a constant and cold temperature T'_C. It is assumed that a forced flow enters the channel with a uniform velocity u'_0. Using the hypothesis of an incompressible laminar flow of a Newtonian fluid (air) obeying the Boussinesq approximation, the dimensionless equations governing this problem, written in the stream function-vorticity formulation, are:

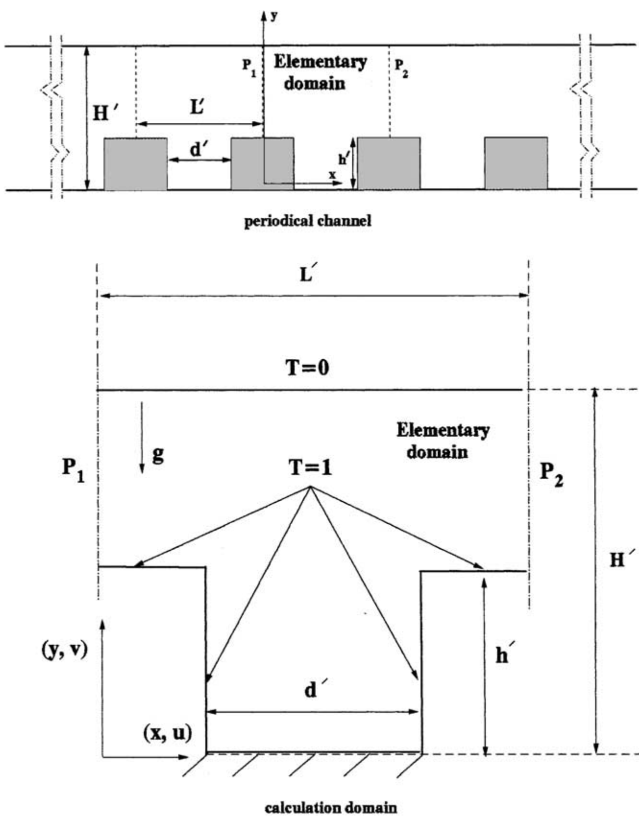

Fig. 1. Schematic of the system studied.

$$\frac{\partial \Omega}{\partial t}+\frac{\partial(u\Omega)}{\partial x}+\frac{\partial(v\Omega)}{\partial y}=-\frac{Ra}{RePe}\left(\frac{\partial T}{\partial x}\right)+\frac{1}{Re}\left(\frac{\partial^2\Omega}{\partial x^2}+\frac{\partial^2\Omega}{\partial y^2}\right) \tag{1}$$

$$\frac{\partial T}{\partial t}+\frac{\partial(uT)}{\partial x}+\frac{\partial(vT)}{\partial y}=\frac{1}{Pe}\left(\frac{\partial^2 T}{\partial x^2}+\frac{\partial^2 T}{\partial y^2}\right) \tag{2}$$

$$\frac{\partial^2\Psi}{\partial x^2}+\frac{\partial^2\Psi}{\partial y^2}=-\Omega \tag{3}$$

$$u=-\frac{\partial\Psi}{\partial y} \quad \text{and} \quad v=\frac{\partial\Psi}{\partial x} \tag{4}$$

The boundary conditions associated to Eqs. (1)–(4) are characterized by the no-slip of the fluid particles on the rigid boundaries and the impermeability of the latter ($u = v = 0$ on these boundaries). The remaining conditions are:

- $T = 1$ on the heated blocks,
- $T = 0$ on the upper wall of the channel,
- $\partial T/\partial n = 0$ on the adiabatic surfaces (n being the normal to the considered surface),
- $\Psi = 0$ and -1 on the lower (including the blocks) and upper rigid boundaries, respectively.

Periodic conditions are applied to the fictitious boundaries of the computation domains P_1 and P_2; they are defined as $\Gamma(x, y, t) = (x + A, y, t)$. Here, Γ stays for T, Ψ or Ω.

The mean quantity of heat leaving the system through the cold wall is evaluated as:

$$Q=-\int_0^1 \left.\frac{\partial T}{\partial y}\right|_{y=1} \mathrm{d}x \tag{5}$$

3. Numerical method

Due to the periodic nature of the geometry under consideration, the calculations were restricted to the elementary domain shown in Fig. 1 (Bilgen et al., 1995). In a previous study dealing with natural convection flows in the same geometry, Amahmid et al. (1997) demonstrated that there exist situations where the calculation domain effect must be taken into account. However, the effect of the calculation domain is not considered here since the main objective of this study is rather to illustrate the effect of the interaction between the forced and natural convection on the flow structure and the heat transfer. The conservation equations, Eqs. (1)–(3), governing this problem were solved numerically using a second-order upwind finite difference method to avoid computational instabilities often encountered in this kind of problems at large values of Re when the central differencing scheme is used. Values of the stream function at all grid points were obtained with Eq. (3) via a point successive over-relaxation method. The effect of the grid size on the results was studied using uniform grids of 41×41, 61×61 and 81×81 for $B = 1/2$ and 1/4 while for $B = 1/8$, grids of 41×41, 65×65 (since a uniform grid of 61×61 does not yield nodes on the upper surface of the blocks) and 81×81 were tested. The tests performed in the case of $B = 1/2$ showed that a grid of 41×41 or 61×61 (depending on Ra and Re) is sufficient for the range of parameters considered in this problem. Examples of these tests are given in Tables 1 and 2. Table 1 shows that for $(Ra, Re) = (10^4, 0.5)$ and (10^5, 0.8) the heat transfer induced by a grid of 41×41 differs by less than 3% from that induced by a grid of 81×81. Concerning ψ_{max} and ψ_{min} (which characterize the intensities of positive and negative cells), satisfactory results are obtained by a grid of 41×41 if one excepts the value $\psi_{max} = 2.76$ obtained in the case of $(Ra, Re) = (10^4, 0.5)$ and which differ by 8% from that corresponding to the grid of 81×81 ($\psi_{max} = 3.0$). In fact it was found that this difference has not a significant effect on the qualitative behavior of the flow. For $(Ra, Re) = (5 \times 10^5, 1.8)$ the heat transfer induced by a grid of 41×41 differs by about 6% from that corresponding to the mesh of size 81×81. The difference in terms of ψ_{max} is close to 6%. With a grid of 61×61 these differences become less than 2.5%, which implies that a grid of 61×61 is more appropriate for this case. Table 2 illustrates the effect of the grid size on the critical

Table 1
Effect of the grid size on the characteristics of heat transfer and fluid flow for $B = 1/2$ and various Ra and Re

Grid	$Ra = 10^4$ and $Re = 0.5$		$Ra = 10^5$ and $Re = 0.8$		$Ra = 5 \times 10^5$ and $Re = 1.8$	
41×41	$Q = 2.029$	$\psi_{max} = 2.76$ $\psi_{min} = -2.18$	$Q = 5.30$	$\psi_{max} = 18.55$ $\psi_{min} = -15.31$	$Q = 9.21$	$\psi_{max} = 16.92$ $\psi_{min} = -22.47$
61×61	$Q = 2.027$	$\psi_{max} = 2.92$ $\psi_{min} = -2.25$	$Q = 5.21$	$\psi_{max} = 19.05$ $\psi_{min} = -15.88$	$Q = 8.86$	$\psi_{max} = 17.56$ $\psi_{min} = -22.80$
81×81	$Q = 2.027$	$\psi_{max} = 3.00$ $\psi_{min} = -2.29$	$Q = 5.18$	$\psi_{max} = 19.32$ $\psi_{min} = -16.18$	$Q = 8.67$	$\psi_{max} = 17.93$ $\psi_{min} = -23.06$

Table 2
Effect of the grid size on Re_{cr} for $B = 1/2$ and various Ra

Grid	$Ra = 10^5$	$Ra = 5 \times 10^5$
41×41	$Re_{cr} = 0.9$	$Re_{cr} = 1.9$
61×61	$Re_{cr} = 0.8$	$Re_{cr} = 1.8$
81×81	$Re_{cr} = 0.8$	$Re_{cr} = 1.8$

Reynolds numbers, Re_{cr}, characterizing the appearance of unsteady convection. It can be seen from this table that satisfactory results can be obtained using a grid of 61×61. Similar tests were performed in the case of $B = 1/4$ and 1/8 but the results are not presented here for reason of brevity. For these two values of B, it is found that a grid of 41×41 (compared with 81×81) gives satisfactory results in most of the situations considered in this study. For the other situations where this grid was estimated not sufficient (although it gives satisfactory qualitative results), grids of 61×61 for $B = 1/4$ and 65×65 for $B = 1/8$ were used instead. It should be mentioned that, at relatively high values of Re for which the flow is dominated by forced convection, a grid of 41×41 was found sufficient for the evaluation of the heat transfer in the channel in the sense that it leads to results slightly different (from a quantitative point of view) from those obtained with a grid of 81×81. However, by increasing Ra, the grid of 41×41 may cause a very slight decrease of the heat transfer (which is not physical) instead of a very slight increase observed with a grid of 81×81. For the temporal discretization, time steps between 10^{-5} and 10^{-4} were considered.

4. Results and discussion

In the following sections, flow and temperature fields, heat transfer rates and the parameters characterizing the displacement of the convective cells (when the latter are moving) are examined for $A = L'/H' = 1$, $C = d'/H' = 0.5$, $0.25 \leqslant B = h'/H' \leqslant 0.5$, $Pr = 0.71$ (air), $10^4 \leqslant Ra \leqslant 10^6$ and $0.1 \leqslant Re \leqslant 200$.

4.1. Case of $B = 1/2$

As it was demonstrated in the past by Hasnaoui et al. (1991) in the case of a channel periodically heated from below, the steady-state transverse cells are displaced downstream when the Reynolds number exceeds some critical value. In the present study, two steady solutions have been obtained before the displacement of the cells occurs. The streamlines and isotherms for these solutions are illustrated in Fig. 2a and b for $Ra = 5 \times 10^4$ and $Re = 0.5$. It can be seen that the path of the forced flow is strongly deformed by the strength of the natural convection cells. As a result, the forced flow enters the domain from the bottom (Fig. 2a) or the top (Fig. 2b) depending on whether the natural convection cell located at the entrance is clockwise or counter-clockwise rotating (the forced flow circulates above the positive cell and below the negative one). Note that, despite the different behaviors exhibited by the forced flow in Fig. 2a and b, these two solutions engender nearly the same quantity of heat leaving the system through the cold wall. However, they locally induce different thermal behaviors (and thereby different local heat transfers) around the corners of the heating blocks (compare for instance the isotherms of Fig. 2a and b). It should be mentioned that a symmetric bicellular pattern is also possible for this problem (Amahmid et al., 1997) but the latter is destroyed by the forced flow even at Re as low as 0.1 and this in favor of one of the two asymmetric solutions of Fig. 2a and b. When Re exceeds some critical value, Re_{cr}, which increases with Ra (Fig. 3), the flow becomes unsteady and the natural convection cells are carried downstream by the forced flow. The variations with time of the maximum stream function, ψ_{max}, and its position, X_{max}, in the domain (X_{max} indicates the position of the center of the most intense positive cell) when the convective cells are moving in the channel, are illustrated in Fig. 4a and b for $Ra = 2 \times 10^5$ and $Re = 1.3$. It can be seen that ψ_{max} and X_{max} exhibit periodic variations with time (the period is close to 1.21). The complex variations observed in the case of ψ_{max} are due to the complex transformations undergone by the convective cells during their displacement as it is illustrated in Fig. 5. In these figures, the streamlines and the isotherms are presented at selected instants of the flow cycle. A close inspection of Fig. 4a and b shows that, in general, the maximum values of ψ_{max} are obtained for X_{max} in the vicinity of $x = 0.5$. This corresponds to situations where the positive cell arrives above the

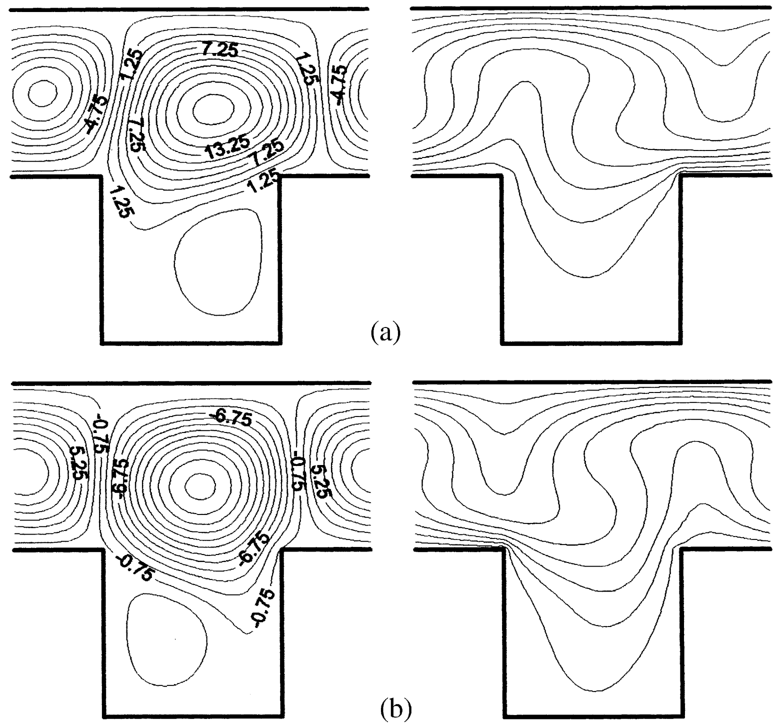

Fig. 2. Streamlines (left) and isotherms (right) for two steady solutions obtained with different initial conditions in the case of $B = 1/2$, $Ra = 5 \times 10^4$ and $Re = 0.5$.

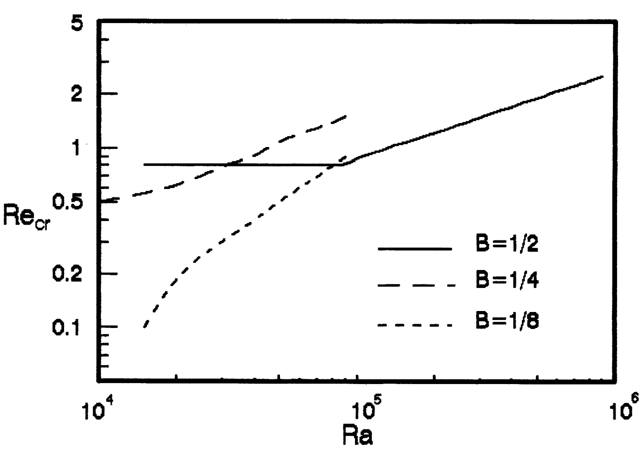

Fig. 3. Re_{cr} versus Ra for various B.

microcavity. However, the minimum values of this quantity are obtained when the positive cell is above the blocks (i.e. when it is submitted to the shrinking resulting from the height of the blocks and the friction at the level of their upper surfaces). From the time variations of X_{max}, it can be deduced that the dimensionless velocity with which the center of the positive cell is moving depends on time. For example, its mean values for the ranges $0.05 \leqslant X_{max} \leqslant 0.1$, $0.20 \leqslant X_{max} \leqslant 0.5$ and $0.7 \leqslant X_{max} \leqslant 1$ are 0.1, 3.95 and 2.7, respectively, while the mean velocity over the entire domain ($0 \leqslant X_{max} \leqslant 1$) is equal to 0.83. Note that in the case of a dominating forced convection, the external flow occupies the space above the blocks and its dimensionless mean velocity in this region is 2 (for $B = 1/2$). This implies that the velocity of the moving cells can be higher than that of the mean forced flow during some time intervals of the flow cycle. As an example, for the range $0.2 \leqslant X_{max} \leqslant 0.5$, the mean velocity of the positive cell is nearly twice that of the forced flow. However, the mean velocity of the cells over the entire domain is lower than that of the forced flow. It can be seen from Fig. 5 that the forced flow is restricted to a very narrow band in the domain and its path is still controlled by the natural convection cells. This means that the displacement of the cells is not due to the dominance of the forced flow but it results from an interaction between the forced and free convection phenomena. It is interesting to note that, at relatively small Ra, the flow remains steady when Re is progressively increased from its lowest value 0.1 (considered here), but the size of the natural convection cells decreases until their complete disappearance. The flow structures induced in this geometry (Fig. 5) are very different from those observed by Hasnaoui et al. (1991) while studying the mixed convection in a channel without blocks. The difference is mainly due to the presence of non-travelling secondary cells in the microcavity of the present geometry. Fig. 5a shows that the main positive cell is located at the entrance of the domain and the secondary positive one in the vicinity of the left corner of the microcavity. During the evolution of the cycle, the

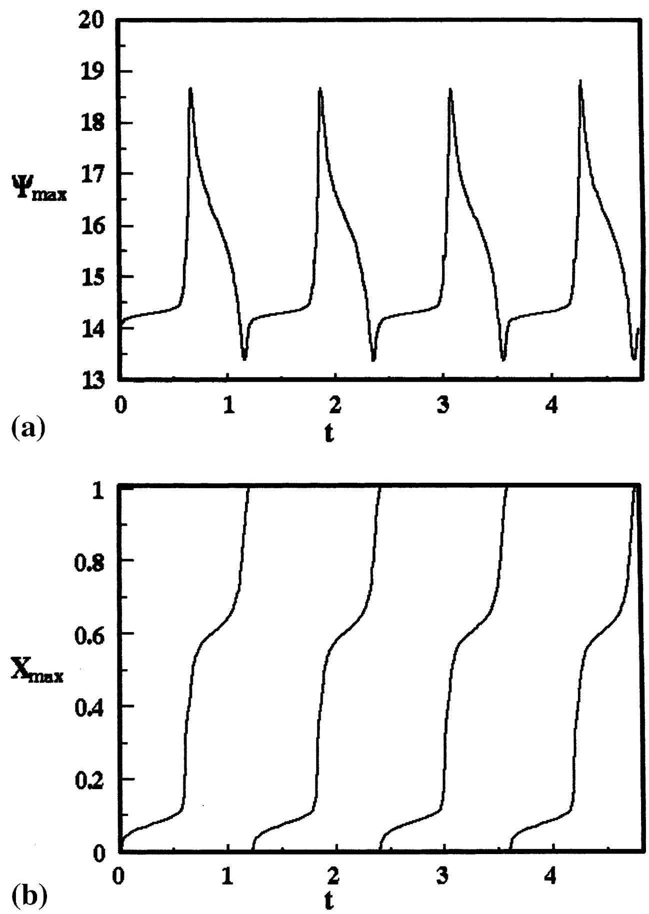

Fig. 4. Variations of Ψ_{max} (a) and X_{max} (b) with time for $B = 1/2$, $Ra = 2 \times 10^5$ and $Re = 1.3$.

main positive cell is displaced downstream until it mixes with the secondary positive one located in the microcavity (Fig. 5b). In the same way, the negative cell, while being shifted also downstream, mixes with the small negative cell located in the lower right corner of the microcavity and the new negative cell thus formed expands progressively to the detriment of the positive cell as it can be seen from Fig. 5b and c. The combined effects of the cells displacement and the transformation they undergo lead to the structure of Fig. 5c where the flow is nearly symmetric with respect to the vertical centerline of the domain while the forced flow is allowed to penetrate deeply into the microcavity. After the short establishment of this quasi-symmetry (Fig. 5c), the upper parts of the negative and positive cells are pushed downstream until they break up (at different instants) which leads to the formation of two small cells in the microcavity (Fig. 5d). For the rest of the cycle, the recirculating positive cell, located in the left side of the microcavity (not visible in Fig. 5d), increases in size to the detriment of the small negative neighboring cell located in the right side (Fig. 5e) while the main cells continue to be carried by the forced flow until the beginning of a new cycle. It can also be observed that the

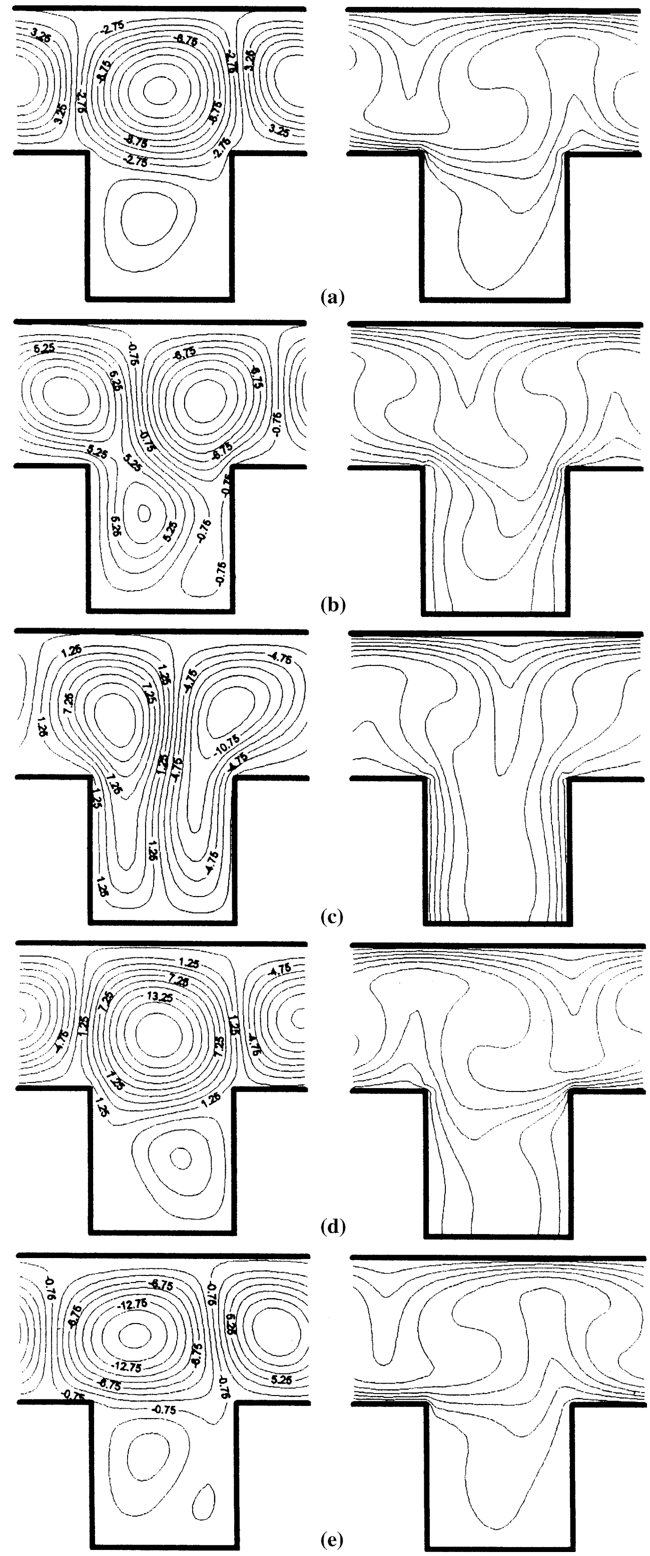

Fig. 5. Streamlines and isotherms at different instants of a flow cycle for $B = 1/2$, $Ra = 2 \times 10^5$ and $Re = 1.3$.

path of the forced flow, which is responsible for the unsteadiness, undergoes considerable changes during one flow cycle. By progressively increasing Re, the forced flow occupies more and more space in the domain. This behavior is illustrated by presenting in Fig. 6a–e streamlines and isotherms at selected instants of the flow cycle obtained for $Ra = 2 \times 10^5$ and $Re = 30$. The size of the natural convection cells are now considerably reduced by the strength of the imposed flow. The positive cell which is moving under the open lines (above the left block in Fig. 6a) exhibits a complex behavior during its evolution with time. In fact, while progressing, it mixes with the secondary positive cell located in the left corner of the microcavity leading to the flow structure of Fig. 6b. The upper part of the new positive cell is inclined by the forced flow towards the right block and its lower part undergoes a shrinking due to the increase of the negative cell size in the right corner of the microcavity (Fig. 6b and c). This situation leads to the division of the positive cell into two small cells (Fig. 6d and e). Note that during some time intervals of the flow cycle, a part of the forced flow penetrates deeply into the microcavity (Fig. 6e). Such a penetration does not occur in the forced convection dominating regime. The variations with time of $X_{\min}$, giving the position of the negative cell located between the open lines and the cold wall, are nearly linear (Fig. 7). This indicates that the negative cell moves with a constant velocity which is close to the mean velocity of the forced flow above the blocks, i.e. 2. Note that the period of the flow cycle is considerably reduced by increasing Re from 1.3 to 30; it drops from 1.21 to 0.46. By further increasing Re, the natural convection cells disappear. Thus, the forced flow occupies the whole space above the blocks inducing a clockwise recirculating vortex in the microcavity and the convection regime becomes steady again.

4.2. Cases of $B = 1/4$ and 1/8

For $B = 1/4$ and 1/8, Amahmid et al. (1997), using a central differencing scheme, demonstrated that the symmetric bicellular flow disappears for some ranges of Ra. However, with the upwind scheme, used in the present study to avoid eventual numerical problems often caused by the central scheme when the forced flow is imposed, it is found that all the steady natural convection solutions are symmetric and bicellular (results not presented). A detailed examination of the effect of the numerical method on the maintenance of such solutions is not performed since the objective here is to investigate the effect of the forced flow on the natural convection solutions. Thus, similarly to the case of $B = 1/2$, it is found that there exists a critical value of Re above which the flow becomes unsteady and the convective cells are moving downstream. The variations of Re_{cr} with Ra are shown in Fig. 3 for different values of B. The evolution of the flow structure and the temperature fields during one flow cycle is presented in Fig. 8 for $B = 1/4$, $Ra = 5 \times 10^4$ and $Re = 1.2$. It can be seen that

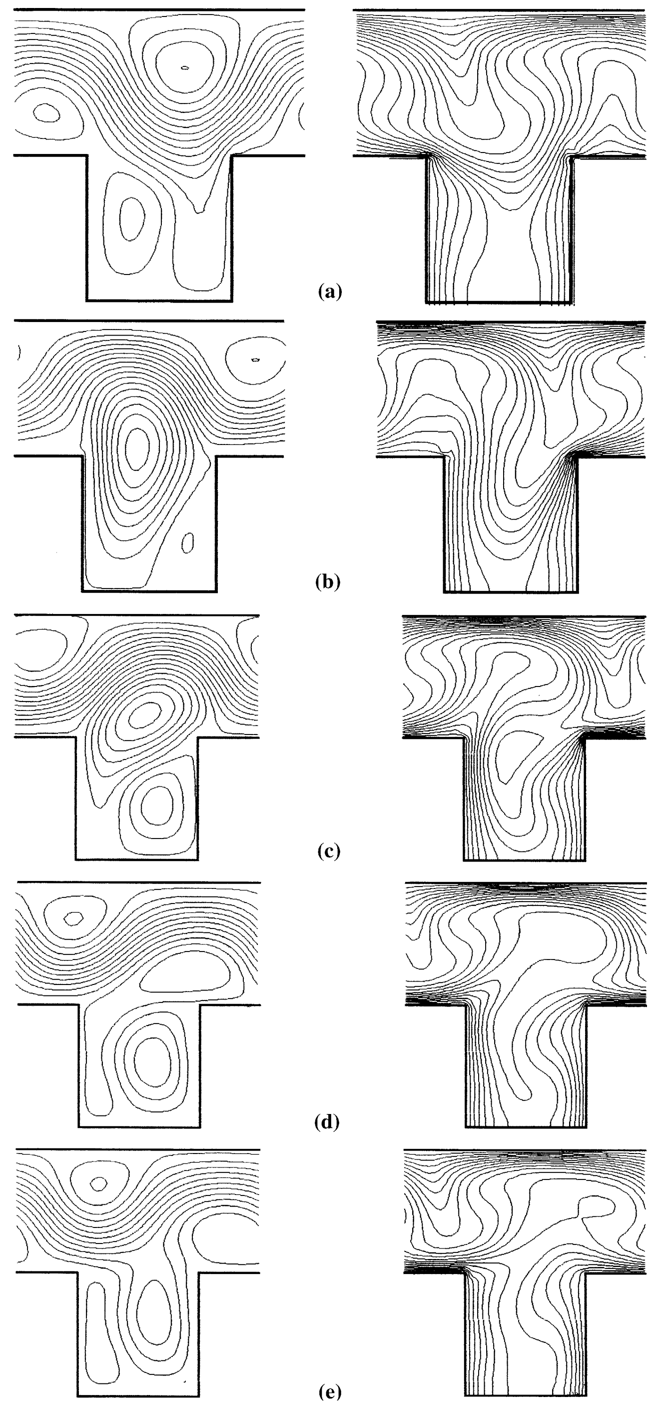

Fig. 6. Streamlines and isotherms at different instants of a flow cycle for $B = 1/2$, $Ra = 2 \times 10^5$ and $Re = 30$.

the flow structure is not notably modified as it is the case for $B = 1/2$. This difference results from the reduction of the blocks height which is not favorable to the development of the secondary cells in the microcavity. The variations of $X_{\max}$ with time, presented in Fig. 9, show that the velocity of the main positive cell is characterized by the existence of two principal regions. In the first

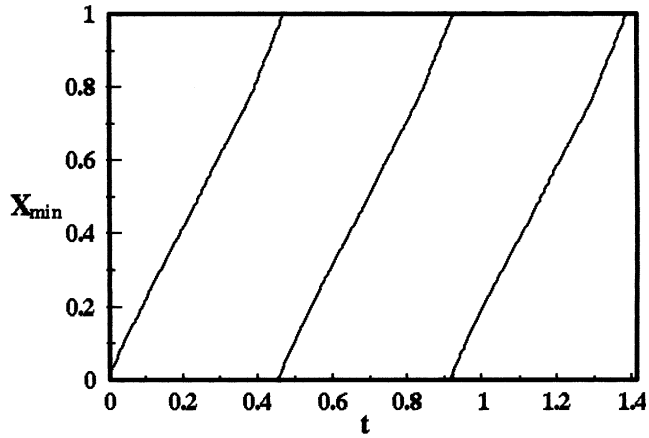

Fig. 7. Variations of $X_{\min}$ with time for $B = 1/2$, $Ra = 2 \times 10^5$ and $Re = 30$.

region ($0 < X_{\max} \leqslant 0.15$) the positive cell is decelerated and the corresponding mean velocity is close to 0.17. In the second region ($0.15 < X_{\max} \leqslant 1$), the cell is accelerated and its mean velocity is about 1.41. Note that in the region where the cell is accelerated, its mean velocity is higher than that of the forced flow calculated above the blocks (the latter is equal to $1/(1 - B) = 4/3$). However, the latter velocity remains higher than the mean velocity of the cells over the entire domain which is close to 0.68.

Let us now reconsider Fig. 3 showing the variations of Re_{cr} with Ra for various values of B. At relatively small values of Ra ($Ra < 2 \times 10^4$), Re_{cr} increases with B since the increase of the blocks height retard the displacement of the convective cells in the channel. However, Re_{cr} corresponding to $B = 1/2$ becomes lower than those corresponding to $B = 1/4$ and 1/8 for Ra higher than 2×10^4 and 8×10^4, respectively. This phenomenon is probably due to the considerable changes undergone by the flow structure in the case of $B = 1/2$ when Ra is increased. In fact, for $B = 1/2$, the flow passes from a symmetric bicellular structure to an asymmetric one with a tendency for the main convective cells to be evacuated from the microcavity when Ra is increased. Consequently, their size becomes smaller and their displacement is facilitated. It is useful to mention that the effect of the grid size on the evolution of Re_{cr} was examined to ensure that the complex behavior exhibited by the curves in Fig. 3 is not due to the grid insufficiency. In addition, for each value of B, only the range of Ra leading to stationary natural convection was considered.

4.3. Heat transfer

Note that the instantaneous global quantity of heat, Q, leaving the system through the cold wall varies periodically with time when the flow becomes unsteady ($Re > Re_{\mathrm{cr}}$). To well characterize the heat transfer, it is useful to consider the mean value of Q (denoted Q_m)

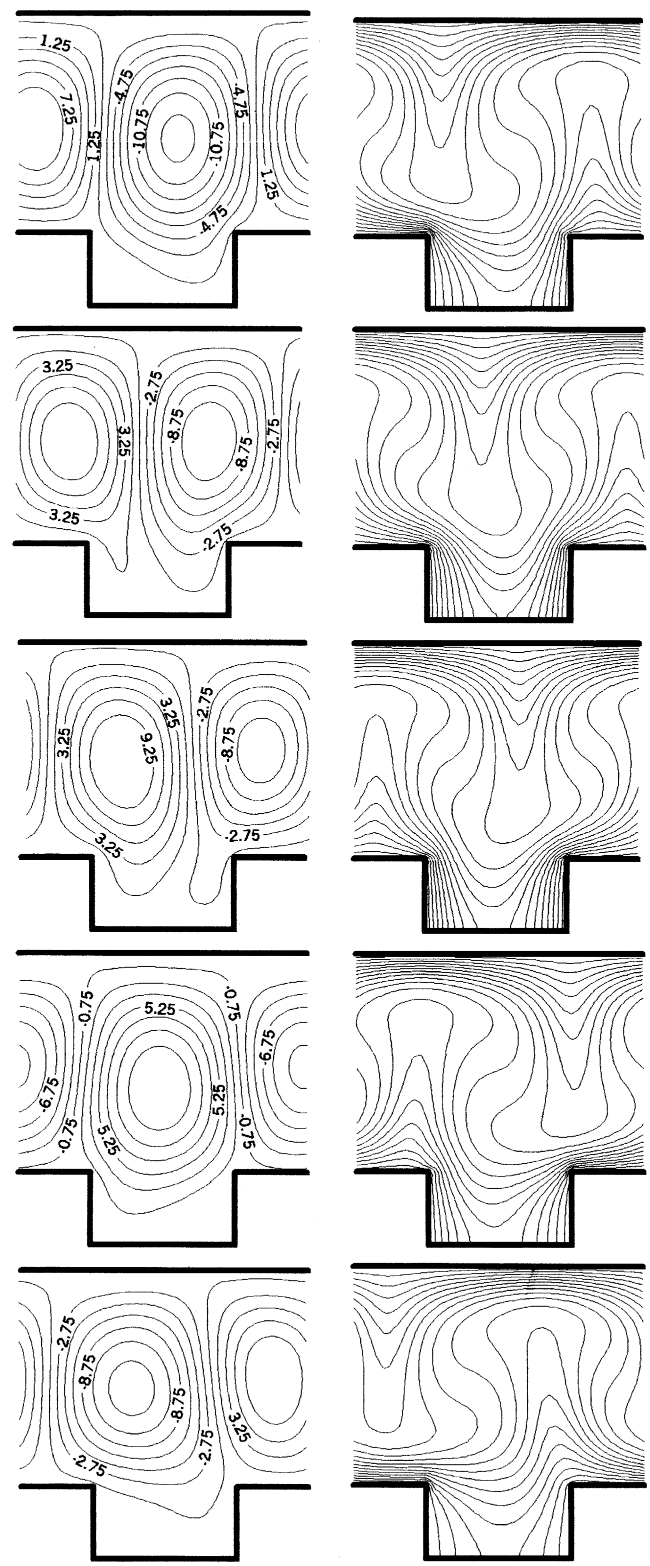

Fig. 8. Streamlines and isotherms at different instants of a flow cycle for $B = 1/4$, $Ra = 5 \times 10^4$ and $Re = 1.2$.

over one period of the flow. The effect of Re on Q_m is presented in Fig. 10a and c for different values of B and Ra. It was observed that the displacement of the cells

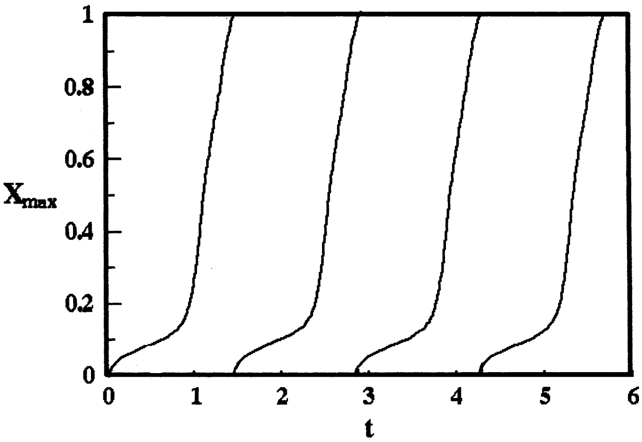

Fig. 9. Variations of $X_{\max}$ with time for $B = 1/4$, $Ra = 5 \times 10^4$ and $Re = 1.2$.

does not affect considerably the mean quantity of heat evacuated through the cold wall when Re is slightly higher than Re_{cr}. However, it can be deduced from Fig. 5c that the fluid is allowed to flow from the microcavity towards the cold wall during some time intervals of the flow cycle. In such situations, the heat transfer from the vertical faces of the blocks is expected to be more important than that corresponding to the steady flow at sufficiently high Ra where the fluid flow in the microcavity consists of small vortices which prevents the exchange of air between the microcavity and the cold region.

For $B = 1/2$, Fig. 10a shows that, in general, Q_m decreases monotonically with Re towards a quasi-asymptotic value corresponding to a dominated forced convection regime. The heat transfer reduction induced by the forced flow is more pronounced at high Ra. As indication, Q_m is divided by about 3 at $Ra = 10^5$ when Re passes from 0 to 80. In fact, the forced flow, which is fully developed, enters and leaves the domain with the same mean temperature (periodic conditions), without inducing any convective heat transport in the horizontal direction. Furthermore, the natural convection cells engender a permanent circulation of the fluid between the hot and cold walls leading to an enhancement of the convective heat transfer in the channel. The imposition of a horizontal forced flow in the channel has a tendency to weaken the vertical flow induced by natural convection cells. Consequently, the heat transfer by convection is reduced. Note that this behavior is related only to the periodic fully developed flow, i.e. far from the entrance region. Similar tendencies are observed for $B = 1/4$ and 1/8. The quasi-asymptotic value obtained for Q_m at large values of Re (i.e. when the flow becomes steady and dominated by the forced convection) is not very different from those corresponding to purely conductive regime. For the results presented in Fig. 10, the values of Q_m corresponding to $Re = 200$ (for instance) exceed those of

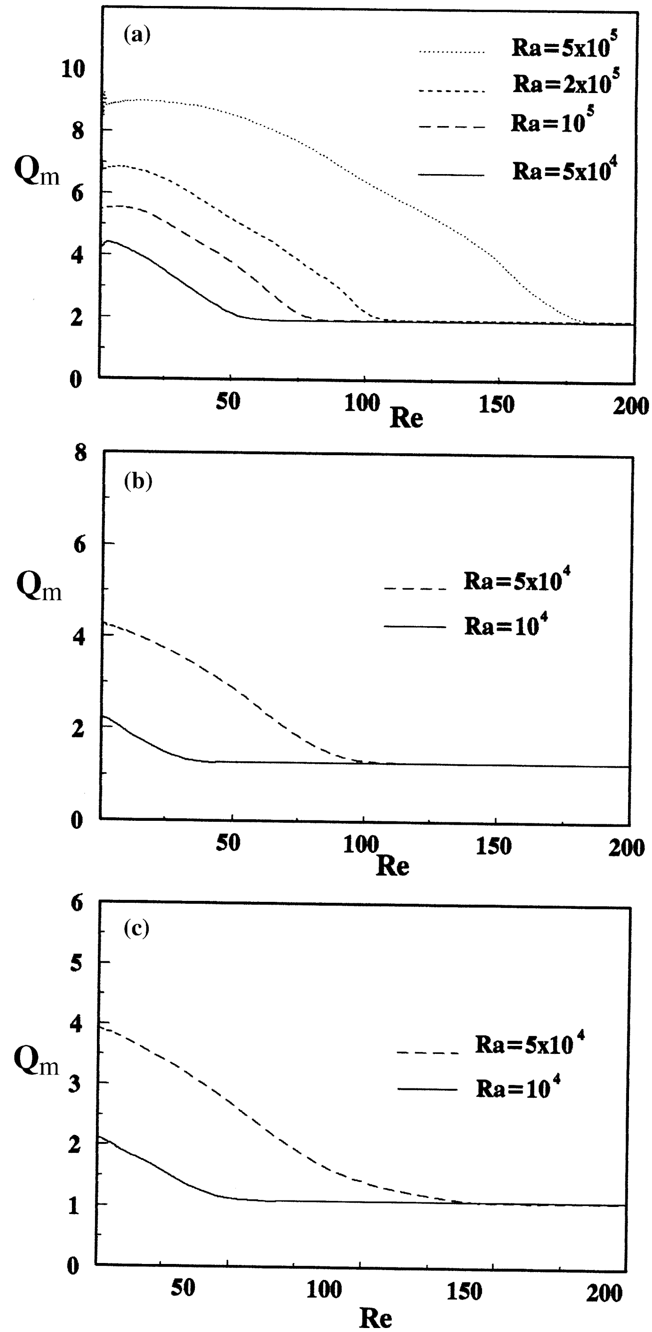

Fig. 10. Q_m variations versus Re for various Ra and B: (a) $B = 1/2$, (b) $B = 1/4$ and (c) $B = 1/8$.

the pure conduction regime ($Re = Ra = 0$) by only 1.4%, 1.6% and 4.9% for $B = 1/8$, 1/4 and 1/2, respectively. It should be mentioned that, at high values of Re, the forced flow which is nearly horizontal, tends to impose a temperature $T \approx 1$ at the opening of the microcavity (plane $y = B$) since the fluid moving in the neighborhood of this plane has already been in contact with the heated blocks. Furthermore, the flow becomes horizontal above this plane ($y = B$) without inducing any heat transfer in the downstream direction. As a result, the quasi- asymptotic value of Q_m is expected to be close to the one that would be induced by pure conduction between the hot wall (maintained at $T = 1$) located at $y = B$, and the cold wall located at $y = 1$, which is $Q_m = 1/(1 - B)$. For example, at $Re = 200$ and $Ra < 10^5$, Q_m is close to 1.10, 1.29 and 1.94 for $B = 1/8$, 1/4 and 1/2, respectively. Such values differ from those predicted by the previous relation of Q_m by less than 4%.

5. Conclusion

Mixed convection in a horizontal channel containing heated blocks on its lower wall is studied numerically. It is demonstrated that there exists a critical *Re* above which the natural convection cells are carried downstream by the forced flow. The displacement of the cells can be observed even in situations where the flow is dominated by natural convection. The fluid flow evolution is periodic in time during the cells displacement and the instantaneous velocity of the latter is function of time. Sometimes, this velocity exceeds largely the mean velocity of the forced flow. At large values of *Re*, the natural convection cells vanish and the heat transfer in the channel is consequently reduced. At relatively small *Re* (even for *Re* slightly higher than Re_{cr}), the unsteady flow is found to favor the ventilation of the vertical faces of the blocks which leads to a better participation of these faces to the heat transfer.

References

Amahmid, A., Hasnaoui, M., Vasseur, P., 1997. Multiplicité des solutions en convection naturelle dans une géométrie répétitive. Int. J. Heat Mass Transfer 40, 3805–3818.

Bilgen, E., Wang, X., Vasseur, P., Meng, F., Robillard, L., 1995. On the periodic conditions to simulate mixed convection heat transfer in horizontal channels. Num. Heat Transfer, Part A 27, 461–472.

Braaten, M.E., Patankar, S.V., 1985. Analysis of laminar mixed convection in shrouded arrays of heated rectangular blocks. Int. J. Heat Mass Transfer 28, 1699–1709.

Fusegi, T., 1996. Mixed convection in periodic open cavities with oscillatory throughflow. Num. Heat Transfer, Part A 29, 33–47.

Hasnaoui, M., Bilgen, E., Vasseur, P., Robillard, L., 1991. Mixed convective heat transfer in a horizontal channel heated periodically from below. Num. Heat Transfer, Part A 20, 297–315.

Kennedy, K.J., Zebib, A., 1983. Combined free and forced convection between horizontal parallel plates. Int. J. Heat Mass Transfer 26, 471–474.

Kim, S.Y., Sung, H.J., Hyun, J.M., 1992. Mixed convection from multiple-layered boards with cross-streamwise periodic boundary conditions. Int. J. Heat Mass Transfer 35, 2941–2952.

Tomimura, T., Fujii, M., 1987. Laminar mixed convection heat transfer between parallel plates with localized heat sources. Proc. Int. Symp. Cooling Technology for Electronic Equipment, Honolulu, pp. 233-247.

Wu, H.W., Perng, S.W., 1998. Heat transfer augmentation of mixed convection through vortex shedding from an inclined plate in a vertical channel containing heated blocks. Num. Heat Transfer, Part A 33, 225–244.

Yücel, C., Hasnaoui, M., Robillard, L., Bilgen, E., 1993. Mixed convection heat transfer in open ended inclined channels with discrete isothermal heating. Num. Heat Transfer, Part A 24, 109–126.